Author(s): Uusitalo, Juha; Sarén, Jan; Juutinen, Sakari; Leino, Matti; Eeckhaudt, Sarah; Grahn, Tuomas; Greenlees, Paul; Jakobsson, Ulrika; Jones, Peter; Julin, Rauno; Ketelhut, Steffen; Leppänen, Ari-Pekka; Nyman, Markus; Pakarinen, Janne; Rahkila, Panu; Scholey, Catherine; Semchenkov, A.; Sorri, Juha; Steer, Andrew; Venhart, Martin

Title: Alpha-decay studies of the francium isotopes 198Fr and 199Fr nuclei

Year: 2013

Version:

Please cite the original version:

Uusitalo, J., Sarén, J., Juutinen, S., Leino, M., Eeckhaudt, S., Grahn, T., Greenlees, P., Jakobsson, U., Jones, P., Julin, R., Ketelhut, S., Leppänen, A.-P., Nyman, M., Pakarinen, J., Rahkila, P., Scholey, C., Semchenkov, A., Sorri, J., Steer, A., & Venhart, M. (2013). Alpha-decay studies of the francium isotopes 198Fr and 199Fr nuclei. Physical Review C, 87(6), Article 064304. https://doi.org/10.1103/PhysRevC.87.064304

α-decay studies of the francium isotopes ^{198}Fr and ^{199}Fr

J. Uusitalo,[1] J. Sarén,[1] S. Juutinen,[1] M. Leino,[1] S. Eeckhaudt,[1] T. Grahn,[1] P. T. Greenlees,[1] U. Jakobsson,[1] P. Jones,[1] R. Julin,[1] S. Ketelhut,[1,*] A.-P. Leppänen,[1,†] M. Nyman,[1] J. Pakarinen,[1] P. Rahkila,[1] C. Scholey,[1] A. Semchenkov,[2,‡] J. Sorri,[1] A. Steer,[1] and M. Venhart[1,§]

[1]*Department of Physics, University of Jyväskylä, P. O. Box 35, FI-40014 Jyväskylä, Finland*

[2]*Gesellschaft für Schwerionenforschung, D-64220 Darmstadt, Germany*

(Received 30 November 2012; revised manuscript received 8 April 2013; published 10 June 2013)

Very neutron deficient francium isotopes have been produced in fusion evaporation reactions using ^{60}Ni ions on ^{141}Pr targets. The gas-filled recoil separator RITU was employed to collect the fusion products and to separate them from the scattered beam. The activities were implanted into a position sensitive silicon detector after passing through a gas-counter system. The isotopes were identified using spatial and time correlations between the implants and the decays. Two α-particle activities, with $E_\alpha = 7613(15)$ keV and $T_{1/2} = (15^{+12}_{-5})$ ms and $E_\alpha = 7684(15)$ keV and $T_{1/2} = (16^{+13}_{-5})$ ms were identified in the new isotope ^{198}Fr. In addition, the half-life and α-particle energy of ^{199}Fr were measured with improved precision. The measured decay properties deduced for ^{199}Fr and ^{198}Fr suggest that there is an onset of ground-state deformation at $N = 112$ in the Fr isotopes.

DOI: 10.1103/PhysRevC.87.064304 PACS number(s): 23.60.+e, 21.10.Tg, 25.70.Jj, 27.80.+w

I. INTRODUCTION

There are 34 known francium isotopes to date. None of them are stable and the longest living, ^{223}Fr ($T_{1/2} = 22$ min), a child of ^{227}Ac, is the only one occurring in nature. Francium is the most unstable of the first 105 elements in the periodic system. The majority of the francium isotopes are α emitters and α-particle spectroscopy can be employed to extract nuclear structure information.

Not much is known about the low-lying structures in neutron-deficient francium isotopes whereas the situation is better with the corresponding child and grandchild activities. The low-lying structures of neutron-deficient odd-mass bismuth isotopes from ^{187}Bi to ^{203}Bi have the following basic characteristics [1]. The ground state is represented by a spherical $(\pi h^1_{9/2})9/2^-$ configuration, and a moderately oblate $(\pi h^2_{9/2}s^{-1}_{1/2})1/2^+$ intruder state is present at low excitation energies. In the bismuth isotopes the excitation energy of the $1/2^+$ intruder state is coming down as a function of decreasing neutron number and the minimum excitation energy is not reached even when the neutron midshell is crossed at ^{187}Bi. In ^{185}Bi only the $1/2^+$ state has been observed and it was identified to decay by direct proton emission [2,3]. In the odd-mass astatine isotopes the $(\pi h^4_{9/2}s^{-1}_{1/2})1/2^+$ intruder state has been identified in ^{197}At [4], ^{195}At [5], and ^{193}At, ^{191}At [6]. In ^{195}At the $1/2^+$ intruder state becomes the ground state [5] and it persists as the ground state in ^{193}At and ^{191}At [6].

In ^{197}At, the ground state has a spherical $(\pi h^3_{9/2})9/2^-$ configuration. The $9/2^-$ state, being the ground state in odd-mass astatine isotopes, heavier than ^{195}At, has not been observed in the lighter astatine isotopes. In ^{195}At, ^{193}At, and ^{191}At a $7/2^-$ state has been discovered to be the first excited state [5,6]. In the astatine isotopes this state has been seen to decay by α-particle emission and as a result the corresponding low-lying $7/2^-$ states in odd-mass bismuth isotopes ^{191}Bi, ^{189}Bi, and ^{187}Bi have been identified as well [5,6]. The falling trend of excitation energy with decreasing neutron number is also observed for the $(\pi i_{13/2})13/2^+$, single-particle state, in these odd-mass bismuth and astatine nuclei.

In the light odd-mass bismuth and astatine isotopes the above mentioned states are often also discussed in the Nilsson scheme. It is proposed that, when approaching the neutron midshell at $N = 104$, the nucleus is driven to a deformed shape. Then the oblate proton states involved are $1/2^+[400]$, $7/2^-[514]$, $7/2^-[503]$, and $13/2^+[606]$.

It has been demonstrated that intruder states also exist in francium isotopes [7]. An α-decaying $1/2^+$-isomeric state, at 144 keV excitation energy above the $(\pi h^5_{9/2})9/2^-$ ground state in ^{201}Fr, was identified in that study. This was the first time when an $1/2^+$ intruder state was identified in francium isotopes. In odd-mass francium isotopes the $1/2^+$-intruder state has the configuration $(\pi h^6_{9/2}s^{-1}_{1/2})1/2^+$.

The francium isotope ^{199}Fr is the lightest francium isotope known to date [8]. In that study the reported α-decay properties were based on five identified events. No assignment for the spin and parity of the decaying state were given even though the reported decay values point to a favored α decay.

In odd-odd nuclei, α-decay studies have revealed quite complicated spectral structures for which the study of α-decay chains of ^{206}Fr, ^{204}Fr, and ^{202}Fr are excellent examples [7,9]. For these odd-odd isotopes three different α decaying isomeric states with configurations $[\pi(h_{9/2})9/2^- \otimes \nu(i_{13/2})13/2^+]10^-$, $[\pi(h_{9/2})9/2^- \otimes \nu(f_{5/2})5/2^-]7^+$, and $[\pi(h_{9/2})9/2^- \otimes \nu(p_{3/2})3/2^-]3^+$ have

*Present address: TRIUMF, Westbrook Mall, Vancouver V6T2A3, Canada.

†Present address: Radiation and Nuclear Safety Authority STUK, Rovaniemi, Finland.

‡Present address: Fysiskinstitut, University of Oslo, NO-0316 Oslo, Norway.

§Present address: Institute of Physics, Slovak Academy of Sciences, SK-84511Bratislava, Slovakia.

been reported [7,9]. In lighter odd-odd nuclei this picture is affected by down-sloping single particle (proton and neutron) states. For example in a recent study of ^{200}Fr only one α-decaying state was reported [10].

In the present paper new α-decay work on the odd-mass isotope ^{199}Fr is presented. In addition, α-decay properties of the new even-mass isotope ^{198}Fr are obtained.

II. EXPERIMENTAL DETAILS

Heavy-ion induced fusion-evaporation reactions of the type ^{141}Pr(^{60}Ni,xn)$^{201-x}$Fr were used to synthesize neutron deficient francium isotopes in the present work. The ^{60}Ni beam was delivered by the $K = 130$ MeV cyclotron of the Accelerator Laboratory at the Department of Physics of the University of Jyväskylä (JYFL). Energy losses in the retarder foils, in the targets and in the helium gas (70 Pa) of the separator used (see below) were calculated using the TRIM code [11].

Typical ^{60}Ni-beam intensities were 20–60 particle-nA and the total beam on target time was 140 h. The total dose was calculated to be 1.7×10^{17} particles. The bombarding energy in the middle of the target was calculated to be $E_{\rm lab} = 268$ MeV, 5 MeV above the estimated interaction barrier [12]. Rolled ^{141}Pr targets of 1.0 mg/cm^2 thickness, sandwiched between two 50 μg/cm^2 thick carbon foils, were used. By using the mass tables [13] an excitation energy $E^\star$ from 28 MeV up to 39 MeV for the formed compound nuclei was calculated at the back and front of the target, respectively. This amount of excitation favors channels where two or three particles are evaporated. To produce these nuclei in the region were the fissility is very high, it is advantageous to use a target and beam combination in such a way that the final compound nucleus is as cold as possible.

The gas-filled recoil separator RITU [14] was used to separate evaporation residues formed in fusion evaporation reactions from the primary beam and to transport them to the focal plane. In the experiment the GREAT spectrometer [15] was used at the focal plane of RITU (Fig. 1). The GREAT setup consists of one multiwire proportional gas counter (MWPC) and two double-sided silicon strip detectors (DSSD). The silicon strip detectors have 60 vertical and 40 horizontal 1 mm wide strips and the two detectors are placed side by side so that the total width of the detector system is 120 mm. Since the vertical and horizontal position width of each strip is 1 mm the silicon detector can be treated as a pixel detector of 4800 pixels. The time-of-flight (TOF) measured between the gas counter and the silicon detectors combined with the recoil energy deposited in the silicon detectors and the gas counter were used to separate the candidate fusion evaporation products from scattered beam particles. In addition, the gas counter was used to separate the α particles from low-energy recoils. Behind the main silicon detectors a planar Ge detector was used to veto energetic light particles punching through the silicon-strip detector (high-energy signals). The planar Ge detector was also used to measure low-energy γ rays and x rays. In addition, a large Ge-clover detector was used to detect γ rays. Signals from all the detectors were collected employing the triggerless Total Data Readout data-acquisition system [16]. The experiment was monitored online using the GRAIN software package [17].

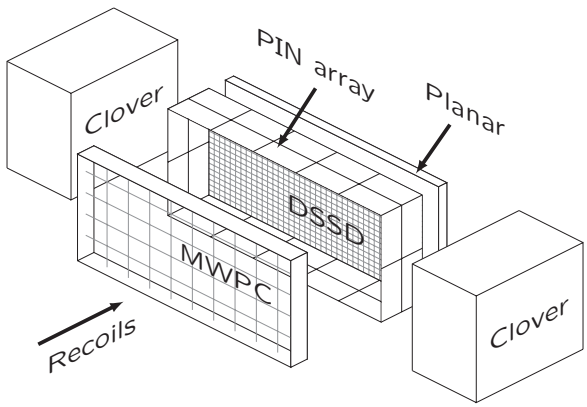

FIG. 1. Schematic view of the focal-plane setup. In the present experiment only one large Ge-clover at the top position was used.

The pressure of the helium filling gas in RITU was 70 Pa. The RITU gas volume was separated from the high vacuum of the beam line using a differential pumping system consisting of a Roots pump and collimators. The counting gas in the MWPC was isobutane of 300 Pa pressure and the counter windows, made of 120 μg/cm^2 Mylar, were also used to keep the silicon detector chamber in high vacuum. The silicon detectors were cooled down to 253 K using circulating alcohol. In the analysis the implants were linked with their subsequent α decays and with α decays of their child nuclei using spatial and temporal correlations.

The DSSD strips were gain matched using well known α activities produced in a separate bombardment where the ^{141}Pr target was replaced with a ^{106}Cd target [18]. For the energy calibration (after gain matching) the α-particle energies were taken from Refs. [19–21] and are 7205(5) keV ^{198}Rn, 7059(10) keV, 6995(10) keV ^{199}Rn^{g,m}, 6850(4) keV, 6754(6) keV ^{198}At^{g,m}, 6844(3) keV ^{194}Po, 6701(4) keV, 6613(7) keV ^{195}Po^{g,m}, 6643(3) keV ^{199}At, and 6520(3) keV ^{196}Po. The full width at half-maximum value with all the vertical 120 strips summed up was measured to be 23 keV at the α-particle energy around 7000 keV.

III. RESULTS

Figure 2(a) presents the energy spectrum of all α particles observed in the silicon detector, vetoed with the gas counter and the planar-Ge detector. The spectrum is dominated by activities formed in fusion channels involving α-particle or proton evaporation. In Fig. 2(b), only α decays correlated within 1 s of an implanted residue inside the proper recoil energy gates are shown. Activities produced involving pure neutron evaporation or one proton in addition to neutron evaporation can be recognized. In Fig. 2(c) the parent-α activities followed by a second α decay within 60 s are shown and finally in Fig. 2(d) the child activities which were preceded by a parent activity are shown. In Fig. 3, a two-dimensional α-energy plot is shown. From the plot different isotopes can be recognized. The astatine isotopes ^{196}At and ^{195}At, produced in

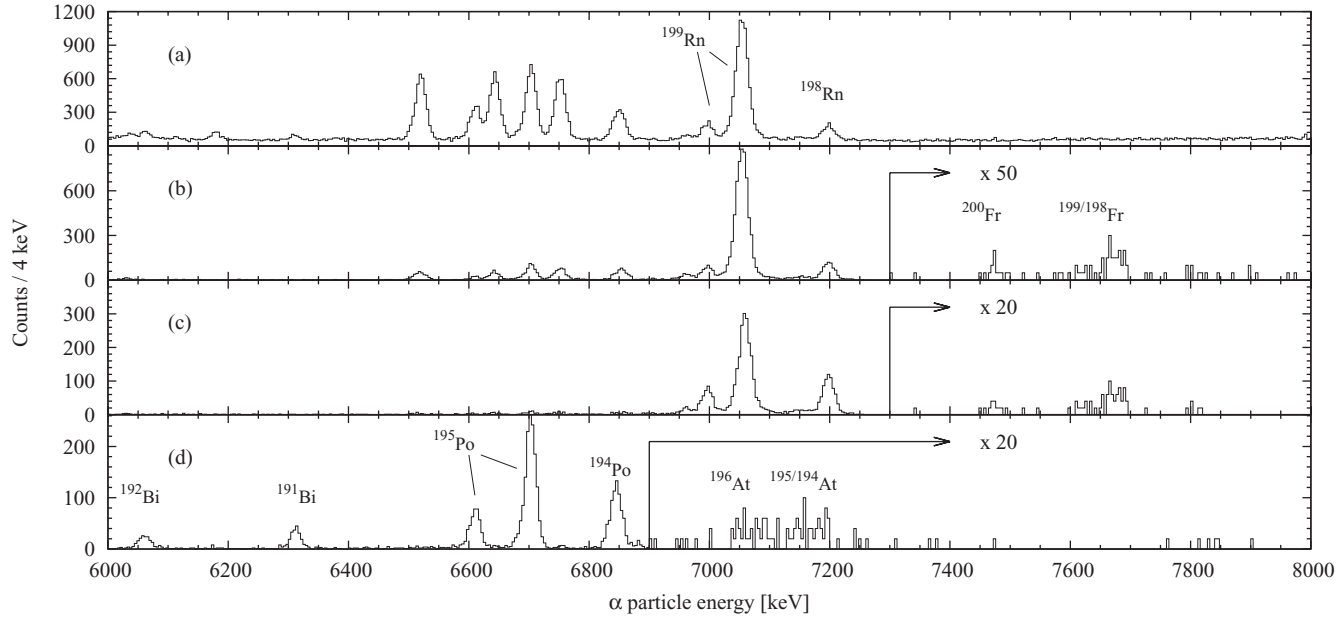

FIG. 2. Energy spectra of α particles measured in the silicon detector and vetoed with the gas counter using the ^{60}Ni + ^{141}Pr reaction: (a) all decays; (b) decays following recoil implants within 1 s; (c) parent decays followed by a second decay within 30 s; (d) child decays following a parent decay.

the αn and $\alpha 2n$ fusion-evaporation channels, respectively, can be identified. In the pn and $p2n$ fusion-evaporation channels the radon isotopes ^{199}Rn and ^{198}Rn were produced. Finally the $1n$, $2n$, and $3n$ fusion evaporation channels yielded the francium isotopes ^{200}Fr, ^{199}Fr, and ^{198}Fr. For the francium isotopes triple α-decay chains, including the child activities

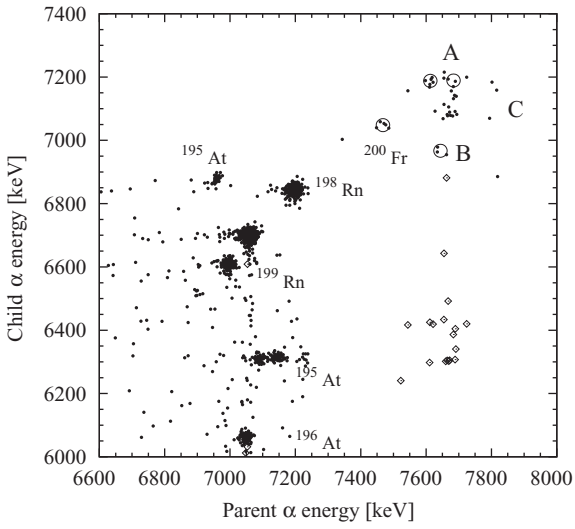

FIG. 3. Parent and child α-particle energies for all chains of the type $ER - \alpha_p - \alpha_c(-\alpha_{gc})$ observed in the ^{60}Ni + ^{141}Pr irradiation. Maximum search times were 1 s for the $ER - \alpha_p$ pair and 60 s for the $\alpha_p - \alpha_c(-\alpha_{gc})$ pair. Dots are for the $\alpha_p - \alpha_c$ pairs and open diamonds represent the $\alpha_p - \alpha_{gc}$ pairs. Some of the identified groups are circled based on the two-sigma confidence level obtained from the ^{198}Rn distribution. Note: From figure it can be seen that in practice all the points are real correlations. The random correlations are expected to show up there where the strongest α 'lines' are crossing.

^{195}At and ^{194}At and grandchild activities ^{191}Bi and ^{190}Bi, were identified as illustrated in Fig. 3. The decay chains, originating from the ^{200}Fr, ^{199}Fr, and ^{198}Fr isotopes, will be discussed in more detail in the following.

Five decay chains were identified where the parent activity with $E_\alpha = 7468(15)$ keV and $T_{1/2} = (37^{+30}_{-12})$ ms was followed by a second decay with $E_\alpha = 7048(12)$ keV and $T_{1/2} = (350^{+290}_{-110})$ ms. The second decay in the chains can be recognized to belong to ^{196}At for which the decay properties with $E_\alpha = 7048(5)$ keV, $T_{1/2} = 388(7)$ ms [22] or with $E_\alpha = 7055(7)$ keV, $T_{1/2} = 300(100)$ ms [23] have been reported. Therefore, the activity with $E_\alpha = 7468(15)$ keV and $T_{1/2} = (37^{+30}_{-12})$ ms can be assigned to ^{200}Fr. These decay values are in good agreement with the recently reported values $E_\alpha = 7473(12)$ keV and $T_{1/2} = 49(4)$ ms for ^{200}Fr [10].

Unambiguous identification of the francium isotopes ^{199}Fr and ^{198}Fr is more difficult. The relative production yields of the radon isotopes ^{199}Rn and ^{198}Rn, produced in pn and $p2n$ evaporation channels, respectively, indicate that the $2n$-evaporation channel has higher yield than the $3n$-evaporation channel. The fact that the decay properties of the corresponding child activities ^{195}At and ^{194}At overlap makes the identification difficult. To justify the division of individual events between the francium isotopes ^{198}Fr and ^{199}Fr the reported decay properties of the child and grandchild activities will be discussed in more detail in the following.

A detailed α-decay spectroscopic study of ^{194}At [24], reports identification of two α-decaying states. A high-spin state was observed to decay with a half-life of 310(8) ms, the main α-decay energy line being 7178 keV (78% branch). Similarly a low-spin state has decay properties of 253(19) ms and 7190 keV (83% branch). In addition, several fine structure lines were identified.

A detailed α-decay study has also been performed for ^{195}At [5]. Two α-decaying states, $1/2^+$ and $7/2^-$, with decay properties of $E_\alpha = 6953(3)$ keV and $T_{1/2} = 328(20)$ ms, $E_\alpha = 7075(4)$ keV, and $T_{1/2} = 147(5)$ ms, respectively, are given. The α decay with $E_\alpha = 7075(4)$ keV was obtained from a broad α-particle energy distribution (7050 keV–7250 keV) which was due to conversion electron summing effects.

The situation is more clear with the grandchild activities ^{190}Bi and ^{191}Bi. For ^{191}Bi two α-decaying states with $I^\pi = 9/2^-$, $E_\alpha = 6308(3)$ keV, $T_{1/2} = 12.4(4)$ s, $I_\alpha = 51(10)\%$ and $I^\pi = 1/2^+$ $E_\alpha = 6870(3)$ keV, $T_{1/2} = 121^{+8}_{-7}$ ms have been obtained [5]. Finally for ^{190}Bi two α-decaying states $I^\pi = 3^+$, $E_\alpha = 6431(5)$ keV, $T_{1/2} = 5.7(8)$ s, $I_\alpha = 90\%$ and $I^\pi = 10^-$, $E_\alpha = 6456(5)$ keV, $T_{1/2} = 5.9(6)$ s, $I_\alpha = 70\%$ have been identified [25].

Based on these decay properties, a first division of events in the group labeled as "A" in Fig. 3, is made based on the decay properties obtained for the grandchild activities. The second decay could then be either a full energy α or an escape. In total, eight triple chains were identified, where the third decay in a chain has the decay properties valid for ^{191}Bi. From those triple chains five child events were obtained with a full α-particle energy. The measured decay properties are $E_\alpha = 7664$ keV, $T_{1/2} = 10$ ms for the parent activity, $E_\alpha = 7081$–7168 keV, $T_{1/2} = 164$ ms for the child activity, and $E_\alpha = 6308$ keV, $T_{1/2} = 13$ s for the grandchild activity.

In total, seven triple chains were identified where the third decay in a chain has decay properties valid for ^{190}Bi. All these chains were obtained with a full α energy for the child decay. These events could be divided into two groups. The first group (five events) has the decay properties $E_\alpha = 7684$ keV, $T_{1/2} = 16$ ms for the parent activity, $E_\alpha = 7189$ keV, $T_{1/2} = 278$ ms for the child activity, and $E_\alpha = 6427$ keV, $T_{1/2} = 9.6$ s for the grandchild activity and the second group (two events) has decay properties $E_\alpha = 7616$ keV, $T_{1/2} = 6$ ms, $E_\alpha = 7180$ keV, $T_{1/2} = 326$ ms, and $E_\alpha = 6422$ keV, $T_{1/2} = 6.3$ s for the parent activity, child activity, and grandchild activity, respectively.

From group A in total 15 events were identified where the two first α decays were found with full energies and where the third decay was an escape or was missing (due to the β decay). From the α-particle energy spectra shown in Refs. [5,24] it can be seen that most of the α-particle energy distribution originating from ^{194}At is centered around 7182 keV whereas there is a wide energy distribution starting from 7050 keV up to 7160 keV identified for ^{195}At. This can be used as a second stage to gain more statistics to obtain decay properties for ^{198}Fr and ^{199}Fr. With an energy window of 7050–7160 keV (and 7200–7300 keV) for the child α, 12 parent α decays can be identified with the decay properties of $E_\alpha = 7672$ keV, $T_{1/2} = 4.9$ ms for the parent activity and $E_\alpha = 7068$–7156 and 7215 keV, $T_{1/2} = 103$ ms for the child activity. This stage also yields three more events for another activity with decay properties $E_\alpha = 7610$ keV, $T_{1/2} = 22$ ms and $E_\alpha = 7193$ keV, $T_{1/2} = 311$ ms for the parent activity and child activity, respectively.

Following this procedure for group A we find 17 events which can be identified to originate from ^{199}Fr and ten events which can be identified to originate from ^{198}Fr. From those 17 events belonging to ^{199}Fr we obtained nine cases where the third α is missing and therefore it can be assumed to be a β decay and similarly in two cases the third α was not found for the chains belonging to ^{198}Fr. From these we get rough β-decay branches of 9/17 and 2/10 for the grandchild activities ^{191}Bi and ^{190}Bi, respectively. These numbers agree well with the β-decay branches given in the literature [5,24].

In two cases, where the second α was grouped to belong to ^{194}At, the obtained child-α particle was in coincidence with a γ-ray events [24]. With the clover-Ge detector a γ-ray event with an energy of 75.0 keV was measured and another one, a γ-ray event with energy of 78.0 keV was obtained with the planar-Ge detector.

All in all the events can be distributed between ^{198}Fr and ^{199}Fr in a quite satisfying way although it cannot be fully ruled out that some events are assigned to the wrong group. After this splitting up of group A two α-decay lines can be obtained for ^{198}Fr with decay values, $E_\alpha = 7684(15)$ keV, $T_{1/2} = (16^{+13}_{-5})$ ms and $E_\alpha = 7613(15)$ keV, $T_{1/2} = (15^{+12}_{-5})$ ms. For ^{199}Fr one α line can be obtained with properties of $E_\alpha = 7668(15)$ keV and $T_{1/2} = (7^{+3}_{-2})$ ms. These decay values measured for ^{199}Fr are well comparable to the values given in literature with $E_\alpha = 7655(40)$ keV and $T_{1/2} = (12^{+10}_{-4})$ ms [8].

Group B consists of three events where the parent activity with $E_\alpha = 7644$ keV and $T_{1/2} = 5.1$ ms was identified to be followed by a second decay with $E_\alpha = 6967$ keV and $T_{1/2} = 428$ ms. One of these chains was identified to be followed by a third decay with $E_\alpha = 6882$ keV and a decay time of 103 ms. The second decay in the chains can be recognized to belong to ^{195}At for which the decay properties with $E_\alpha = 6953(3)$ and $T_{1/2} = 328(20)$ ms [5] have been reported to originate from an isomeric $1/2^+$ proton intruder state. The third decay with $E_\alpha = 6882$ keV in one of the chains can be associated with ^{191}Bi^m for which the decay properties with $E_\alpha = 6870(3)$ keV and $T_{1/2} = (121^{+8}_{-7})$ ms [5] are reported for an isomeric $1/2^+$ proton intruder state. Therefore, the activity with $E_\alpha = 7644$ keV and $T_{1/2} = 5.1$ ms can be justified to originate from ^{199}Fr.

Group C includes four events. In three of them the first α decay is followed by a second α decay which has decay properties consistent with ^{195}At. The individual decay energies for the child events are 7074 keV, 7165 keV, 7190 keV, and $T_{\text{ave}} = 290$ ms. The remaining event is followed by an event for which the decay properties of $E_\alpha = 6885$ keV and decay time of 493 ms are determined. For these four events the α-decay properties $E_\alpha = 7808(20)$ keV and $T_{1/2} = (1.6^{+1.6}_{-0.6})$ ms are obtained. In one case the parent α was in coincidence with a low-energy γ ray. The energy was 80.5 keV obtained with the clover-Ge detector. This value can be compared with the astatine x-ray energy $K_\alpha = 81.5$ keV. As above this activity could be justified to originate from ^{199}Fr.

When the efficiency of the RITU separator is assumed to be 40(10)%, the francium and radon isotopes are estimated to be produced with the following cross sections: ^{199}Fr 240(80) pb, ^{198}Fr 120(50) pb, ^{199}Rn 18(5) nb, and ^{198}Rn 5(2) nb. These cross-section values do not represent the maximum values since excitation functions were not measured and a relatively thick target was used.

TABLE I. The α-decay properties of the francium isotopes and their corresponding child and grandchild isotopes observed in the present work. The literature values are taken from Refs. [6,10]. The α decay reduced widths δ^2 and half-lives normalized to ^{212}Po, calculated according to Ref. [26], are also given. In column 8, the spin and parity of the decaying state are given.

Nuclide	E_α [keV] Meas.	E_α [keV] Lit.	$T_{1/2}$ [ms] Meas.	$T_{1/2}$ [ms] Lit.	$T^\alpha_{1/2}$ [ms] Calc.	δ^2 [keV]	I^π
^{200}Fr	7468(15)	7473(12)	37^{+30}_{-12}	49(4)	30	44(8)	3^+
^{196}At	7048(12)	7048(5)	350^{+290}_{-110}	388(7)	142	27(2)	3^+
^{199}Fr^{m1}	7668(15)	7655(40)	7^{+3}_{-2}	12^{+10}_{-4}	7	80^{+60}_{-30}	
^{195}At^m	7050–7250	7050–7250	130^{+50}_{-30}	147(5)	119	56(4)	$7/2^-$
^{191}Bi^g	6310(10)	6308(3)	(13^{+13}_{-5}) s	12.4(4) s	14 s	41(11)	$9/2^-$
^{199}Fr^g	7644(20)	–	5^{+7}_{-2}	–	9	130^{+120}_{-80}	
^{195}At^g	6967(10)	6953(3)	430^{+590}_{-160}	328(20)	321	71(6)	$1/2^+$
^{191}Bi^m	6882(20)	6870(3)	70^{+340}_{-40}	121^{+8}_{-7}	104	43(7)	$1/2^+$
^{199}Fr^{m2}	7808(20)	–	$1.6^{+1.6}_{-0.6}$	–	2.7	120^{+110}_{-70}	
^{195}At^m	7184, 7159, 7068	7050–7250	200^{+300}_{-80}	147(5)	119	56(4)	$7/2^-$
^{191}Bi^g	6885(15)	6870(3)	340^{+1650}_{-160}	121^{+8}_{-7}	104	43(7)	$1/2^+$
^{198}Fr^{m1}	7613(15)	–	15^{+12}_{-5}	–	11	60^{+40}_{-30}	–
^{194}At^m	7188(12)	7190(15)	320^{+230}_{-90}	253(10)	50	12(2)	–
^{190}Bi^g	6422(10)	6431(5)	(6^{+4}_{-2}) s	5.7(8) s	4.7 s	54(20)	3^+
^{198}Fr^{m2}	7684(15)	–	16^{+13}_{-5}	–	7	30(20)	–
^{194}At^m	7189(12)	7190(15)	280^{+200}_{-90}	253(10)	50	12(2)	–
^{190}Bi^g	6427(10)	6431(5)	(10^{+9}_{-4}) s	5.7(8) s	4.7 s	54(20)	3^+

IV. DISCUSSION

In the present work, α-decay hindrance factors HF (HF = $\delta^2_{ee}/\delta^2_{ue}$) and reduced widths δ^2 ($\delta^2 = \lambda h/P$), calculated according to the Rasmussen formalism [26], are used to obtain structure information of the decaying states. Above δ^2_{ee} denotes to the reduced width of the ground state to ground state decay of the closest even-even case, δ^2_{ue} denotes to the reduced width of the decay under examination, λ is the decay constant, h is Planck's constant, and P is the calculated barrier penetration factor. The α-decay properties of the francium isotopes and their corresponding child and grandchild isotopes observed in the present work are summarized in Table I. The reduced width values shown in Table I are calculated taking into account the α-decay branches given in [13]. If the α-decay branch is not known, a 100% branch is assumed, which is a reasonably good approximation for most of the cases also when considering the predicted β-decay half-life values given in [27].

In this work, three different α-decay lines (energies) were identified for ^{199}Fr. To guide the discussion a speculative α-decay scheme for ^{199}Fr is shown in Fig. 4. According to experimental hindrance factors, all three decays are favored. The child activity ^{195}At was recently studied in an in-beam γ-ray (recoil-decay-tagging) experiment in Jyväskylä [28]. In that work it was noticed that there is a 12(4)% $E3$ branch from the $7/2^-$ excited state to the $1/2^+$ ground state in ^{195}At. In addition, a collective band built on top of the $13/2^+$ state was identified albeit the de-excitation of the $13/2^+$ state remains unknown. This $13/2^+$ state, at $\leqslant$130 keV, probably de-excites by a cascade of $M2$ and $M1$ transitions to the $7/2^-$ state [28]. Hence, it is difficult to firmly determine from which states the three α lines, obtained in this work, originate. Our preferred scenario is given in the following.

The existence of three different α lines suggests that there is a change in the low-energy structure compared to the heavier odd-mass francium isotopes. The α lines could originate from the $1/2^+$, $7/2^-$, and $13/2^+$ states. Since high-spin states are favored in fusion-evaporation reactions the line with α-decay properties $E_\alpha = 7668(15)$ keV, $T_{1/2} = (7^{+3}_{-2})$ ms could originate either from the $7/2^-$ or the $13/2^+$ state. The origin of the second line with α-decay properties $E_\alpha = 7644(20)$ keV, $T_{1/2} = (5^{+7}_{-2})$ ms is not clear either, though it is followed by second and third α decays with decay properties which can be identified to originate from $1/2^+$ states in ^{195}At and ^{191}Bi. Albeit the $1/2^+$ states are weakly populated in heavy ion induced fusion evaporation reactions, the $E3$ branch found in ^{195}At [28] could lead to a conclusion that the α decay with $E_\alpha = 7644(20)$ keV actually is from the same state as the decay with $E_\alpha = 7668(15)$ keV. In total 20 events were attributed to the decay of ^{199}Fr in groups A and B. The $E3$ branch of 12% in ^{195}At gives 2.4 events out of 20 events which is close to the number of events obtained in group B. On the other hand the energy difference of 24 keV between the α lines of 7644 keV and 7668 keV is relatively large pointing to a possibility that the α-particle decay with the energy of 7644 keV (or one or two of the events; note the scattering in the two-dimensional plot) could originate from a different state. The third line with α-decay properties $E_\alpha = 7808(20)$ keV, $T_{1/2} = (1.6^{+1.6}_{-0.6})$ ms was also followed by known α-particle decays from ^{195}At and ^{191}Bi. Since these decay properties differ from those of the other two lines and the obtained coincidence with the astatine x ray it is suggested that this

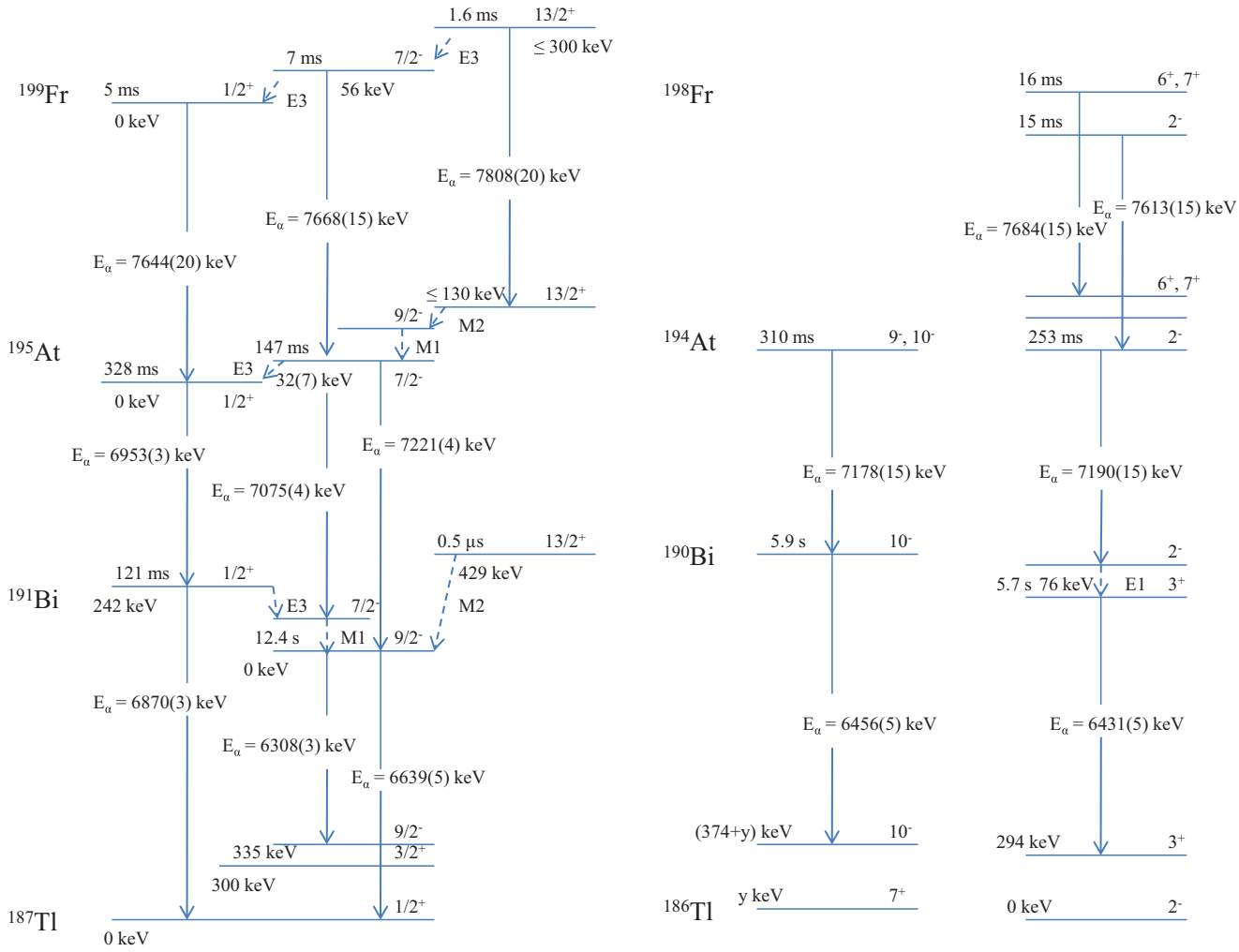

FIG. 4. (Color online) Speculative α-decay schemes for ^{199}Fr and ^{198}Fr are shown.

α-particle decay originates from an another isomeric state decaying to the corresponding state in ^{195}At. If this is the case then the $1/2^+$ state would be the ground state (assuming 7644 keV $1/2^+$ to $1/2^+$ α decay) and the ΔQ value obtained between the α decays with energies 7644 keV and 7668 keV (7808 keV) would be 24 keV pointing to an excitation energy of 56 keV and $\leqslant$300 keV and for the $7/2^-$ and $13/2^+$ states, respectively, in ^{199}Fr. This would mean that there is a possibility for an $E3$ γ-transition branch from the $7/2^-$ state to the $1/2^+$ the (and from the $13/2^+$ state to the $7/2^-$ state) in ^{199}Fr. In another scenario the $13/2^+$ and $7/2^-$ states could be exchanged. Again the $1/2^+$ state would be the ground state but now the $7/2^-$ state would lie at 167 keV and the $13/2^+$ state would be at $\leqslant$150 keV based on α-decay energy differences. In this case competing $E3$ transitions are also expected. However the obtained x-ray coincidence event does not support the latter scenario.

For the even-mass francium isotope ^{198}Fr two α-particle lines were identified. The speculative α-decay scheme for ^{198}Fr is shown in Fig. 4. Both decays were followed by child and grandchild activities, ^{194}At and ^{190}Bi, which in the case of ^{190}Bi was identified to originate from the low-spin state. No clear sign of α-particle decays followed by decays from the high-spin states in ^{194}At and ^{190}Bi were obtained. To make any conclusions, an investigation of the situation in the heavier astatine and francium isotopes is in order. For ^{206}Fr, ^{202}At, ^{204}Fr and ^{200}At three α-particle decaying isomeric states, $[\pi(h_{9/2})9/2^-\otimes\nu(i_{13/2})13/2^+]10^-$, $[\pi(h_{9/2})9/2^-\otimes\nu(f_{5/2})5/2^-]7^+$ and $[\pi(h_{9/2})9/2^-\otimes\nu(p_{3/2})3/2^-]3^+$ have been reported [9]. These states have been suggested to be members of multiplets where single particle or hole proton and neutron states are coupled. The origin of these isomeric states in odd-mass isotopes is rather well reproduced from the known behavior of single-particle states in the neighboring odd-mass nuclei and by applying the parabolic rule [29]. A list of possible configurations and I^π assignments for some of the states are shown in Table II. For ^{202}Fr and ^{198}At only two α-particle decaying isomeric states, $[\pi(h_{9/2})9/2^-\otimes\nu(i_{13/2})13/2^+]10^-$ and $[\pi(h_{9/2})9/2^-\otimes\nu(p_{3/2})3/2^-]3^+$ have been reported [9]. And finally for the pair ^{200}Fr and ^{196}At only one α-particle decaying state, $[\pi(h_{9/2})9/2^-\otimes\nu(p_{3/2})3/2^-]3^+$ has been reported [10]. This can be understood by studying how the single-particle proton and neutron states behave in the

TABLE II. Possible configurations and I^π assignments.

Configuration	Possible I^π	Observed I^π
$\pi(1h_{9/2})\otimes\nu(3p_{3/2})$	$3^+,\ldots,6^+$	3^+
$\pi(1h_{9/2})\otimes\nu(2f_{5/2})$	$2^+,\ldots,7^+$	7^+
$\pi(1h_{9/2})\otimes\nu(1i_{13/2})$	$2^-,\ldots,11^-$	10^-
$\pi(3s_{1/2})\otimes\nu(3p_{3/2})$	$1^-,2^-$	
$\pi(3s_{1/2})\otimes\nu(1i_{13/2})$	$6^+,7^+$	
$\pi(2f_{7/2})\otimes\nu(3p_{3/2})$	$2^+,\ldots,5^+$	
$\pi(2f_{7/2})\otimes\nu(1i_{13/2})$	$3^-,\ldots,10^-$	$9^-,10^-$
$\pi(1i_{13/2})\otimes\nu(3p_{3/2})$	$5^-,\ldots,8^-$	
$\pi(1i_{13/2})\otimes\nu(1i_{13/2})$	$0^+,\ldots,13^+$	

neighboring odd-mass polonium, astatine, radon and francium isotopes. The $13/2^+$ isomeric state in odd-mass polonium and radon isotopes and the $1/2^+$ and the $13/2^+$ isomeric states in odd-mass astatine and francium isotopes are down sloping as a function of decreasing neutron number. At the same time the neutron state $5/2^-$ has an up sloping trend. In the case of ^{200}Fr and ^{198}At, some of the other multiplet members have energies between the 7^+ and 3^+ states, with the result that the 7^+ state is not α-particle decaying anymore. This assumption is supported by the in-beam measurement performed for ^{198}At where almost all the γ-ray transitions identified to feed the α-decaying 10^- isomeric state were also seen in the α-particle decaying 3^+ ground state tagged spectrum [30]. This supports the assumption that there is an $E3$ γ-transition branch to the 7^+ state which is then followed by lower multipolarity γ-ray transitions to the ground state. In the work [22] an isomeric state feeding the 3^+ ground state in ^{196}At was reported. The γ-ray transition was suggested to be a hindered $E2$ transition where the hindrance is due to structural changes. Since no sign of the 10^- state has so far been reported for this nucleus (and neither for ^{200}Fr) it is suggested that some other multiplet members come down between the 10^- isomeric state and the 3^+ ground state allowing the γ-ray transitions to overcome the α-particle decays. Finally the recent α-decay spectroscopy studies of ^{192}At and ^{194}At support this picture [24,31]. In both cases two α-particle decaying isomeric states were identified. In ^{192}At the favoured α-particle decays do not feed the high and low spin states (10^- and 3^+) states in ^{188}Bi directly but instead they feed excited states above these states. The α-particle decay from the high-spin state is followed by an $M1$ γ-ray transition (165 keV) and the α-particle decay from the low spin state is followed by an $E1$ (36 keV) transition. In ^{194}At the α-particle decay from the low-spin state is followed by a 76 keV ($E1$) γ-ray transition. The high-spin states in ^{192}At and in ^{194}At were suggested to have the configuration $[\pi(2f_{7/2})7/2^-\otimes\nu(i_{13/2})13/2^+]9^-,10^-$. The configurations of the low-spin states were also discussed and it was suggested that they could originate from a configuration multiplet $[\pi(s_{1/2})1/2^+\otimes\nu(p_{3/2})3/2^-]1^-,2^-$. These assumptions are supported by the detailed spectroscopic measurements performed for the neighboring odd-mass astatine isotopes ^{191,193,195}At [5,6].

Since no clear sign of α-particle decays feeding the high-spin state in ^{194}At was identified in the present work it is suggested that the two α-particle decays identified in

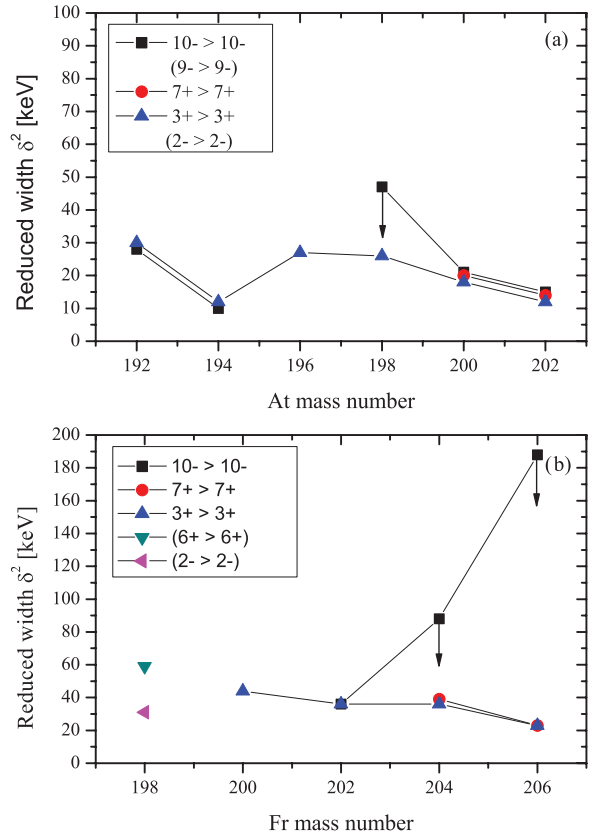

FIG. 5. (Color online) Reduced-width δ^2 values are shown (a) for the even-mass astatine isotopes; (b) for the even-mass francium isotopes. Tentative spin and parity assignments are given in brackets. A down-pointing arrow indicates that there is a competing $E3$ transition, but the $E3$ branch is unknown and a 100% α branch is assumed.

^{198}Fr originate from low(er) spin states. No clear signs of electron summing can be identified and since the decays are favored it is suggested that these two α-particle lines could originate from two different isomeric low-spin states (lower than 9). For example for these states the spin and parity could be 2^- and 7^+ (or 5^+) originating from multiplets $[\pi(s_{1/2})1/2^+\otimes\nu(p_{3/2})3/2^-]1^-,2^-$ and $[\pi(s_{1/2})1/2^+\otimes\nu(i_{13/2})13/2^+]6^+,7^+$ (or $[\pi(f_{7/2})7/2^-\otimes\nu(p_{3/2})3/2^+]2^+,\ldots,5^+$), respectively, and feeding the corresponding states in ^{194}At. On the other hand the two decay times obtained for ^{198}Fr are almost equal which is a sign that there may be only one α-decaying state.

In Figs. 5(a) and 5(b) calculated reduced-width δ^2 values for even-mass astatine and francium isotopes, respectively, are shown. If the α-decay branch is not known an α-decay branch value of 100% is used. Deviations from smooth behavior can be seen in the α decays from the 10^- states in ^{206}Fr, ^{204}Fr, and ^{198}At. In the case of ^{206}Fr and ^{204}Fr there is known to be a competing $E3$ transition but the branching ratios have not been measured. In the case of ^{198}At, as already discussed before, evidence for an existing $E3$ branch was given based on in-beam γ-ray data from Ref. [30]. In these cases the reduced-width values for α decays call for detailed branching-ratio measurements. A deviation from the systematic behavior can also be seen in ^{194}At. It is interesting to note that in those cases

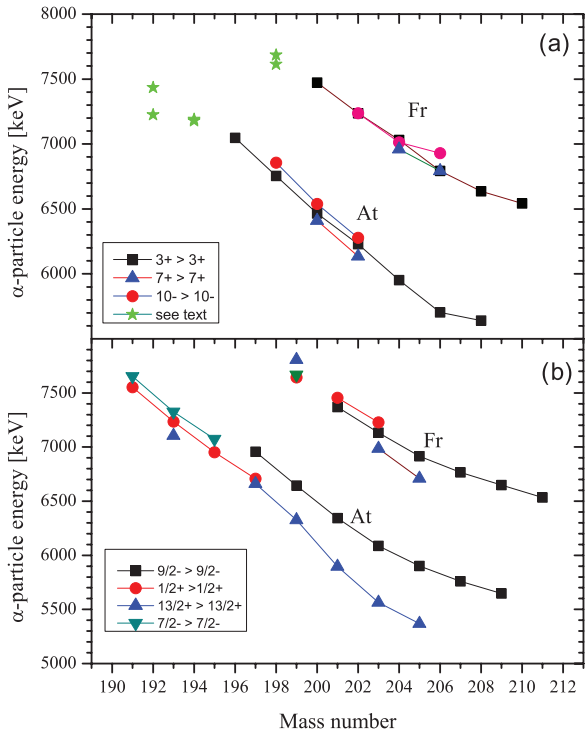

FIG. 6. (Color online) Alpha-energy systematics are shown (a) for the even-mass astatine and francium isotopes; (b) for the odd-mass astatine and francium isotopes.

where the α-decay properties are well known the reduced-width values are remarkably similar for each isotope for α-decays from different isomers.

The above phenomenon can be examined also by looking at the α-decay energy systematics in astatine and francium isotopes. Figure 6(a) shows the α-particle energies for even-mass francium and astatine isotopes whereas Fig. 6(b) shows the α-particle energies for odd-mass francium and astatine isotopes. Only data for the favored decays are shown (and in some cases the α-particle energy is calculated from known level energies). From these data it can be seen that for odd-mass astatine isotopes there is a bend at mass number $A = 197$ in the systematic behavior. This is due to structural changes in the ground states between the parent and child activities. Starting from ^{195}At downward the favoured decays from the ground states feed the corresponding excited states in the child bismuth nuclei. Deviation from the systematics does not occur in the case of francium isotopes. This can be considered as a sign of favored α decays between the ground states.

The mass values given in Ref. [13] for ^{191}Bi and ^{198}Rn and the α-decay value measured for ^{195}At [6] combined with the α-decay value measured for ^{199}Fr in this work can be used to obtain the proton separation value S_p for ^{199}Fr. The obtained value $S_p = -690(30)$ keV implies that even though ^{199}Fr is proton unbound, the proton decay is too slow to noticeably compete with α decay.

In conclusion, a new α-decaying francium isotope ^{198}Fr was identified. Two different α-particle energies were obtained. The francium isotope ^{199}Fr was studied with improved precision. In ^{199}Fr evidence for three different α-decaying states is found. The origin of these decays in ^{199}Fr and in ^{198}Fr was discussed but due to the low number of events no final conclusion could be given. It is also suggested that there is a change in the ground-state configurations starting from ^{199}Fr downwards when compared to the heavier francium isotopes. This suggests an onset of ground-state deformation at $N = 112$ in the francium isotopes.

ACKNOWLEDGMENTS

This work was supported by the Academy of Finland under the Finnish Centre of Excellence Programme 2006–2011 (Nuclear and Accelerator Based Physics Programme at JYFL).

[1] E. Coenen, K. Deneffe, M. Huyse, P. Van Duppen, and J. L. Wood, Phys. Rev. Lett. **54**, 1783 (1985).
[2] C. N. Davids *et al.*, Phys. Rev. Lett. **76**, 592 (1996).
[3] G. L. Poli *et al.*, Phys. Rev. C **63**, 044304 (2001).
[4] E. Coenen *et al.*, Z. Phys. A **324**, 485 (1986).
[5] H. Kettunen *et al.*, Eur. Phys. J. A **16**, 457 (2003).
[6] H. Kettunen *et al.*, Eur. Phys. J. A **17**, 537 (2003).
[7] J. Uusitalo *et al.*, Phys. Rev. C **71**, 024306 (2005).
[8] Y. Tagaya *et al.*, Eur. Phys. J. A **5**, 123 (1999).
[9] M. Huyse, P. Decrock, P. Dendooven, G. Reusen, P. Van Duppen, and J. Wauters, Phys. Rev. C **46**, 1209 (1992).
[10] H. De Witte *et al.*, Eur. Phys. J. A **23**, 243 (2005).
[11] J. F. Ziegler, J. P. Biersack, and U. Littmark, *The Stopping and Range of Ions in Solids* (Pergamon Press, New York, 1985).
[12] R. Bass, Nucl. Phys. A **231**, 45 (1974).
[13] G. Audi, O. Bersillon, J. Blachot, and A. H. Wapstra, Nucl. Phys. A **729**, 3 (2003).
[14] M. Leino *et al.*, Nucl. Instrum. Methods Phys. Res. B **99**, 653 (1995).
[15] R. D. Page *et al.*, Nucl. Instrum. Methods Phys. Res. B **204**, 634 (2003).
[16] I. H. Lazarus *et al.*, IEEE Trans. Nucl. Sci. **48**, 567 (2001).
[17] P. Rahkila, Nucl. Instrum. Methods Phys. Res. A **595**, 637 (2008).
[18] R. D. Page, P. J. Woods, R. A. Cunningham, T. Davinson, N. J. Davis, A. N. James, K. Livingston, P. J. Sellin, and A. C. Shotter, Phys. Rev. C **53**, 660 (1996).
[19] N. Bijnens *et al.*, Phys. Rev. Lett. **75**, 4571 (1995).
[20] F. Calaprice, G. T. Ewan, R.-D. von Dincklage, B. Jonson, O. C. Jonsson, and H. L. Ravn, Phys. Rev. C **30**, 1671 (1984).
[21] A. Rytz, At. Data Nucl. Data Tables **47**, 205 (1991).
[22] M. B. Smith *et al.*, J. Phys. G: Nucl. Phys. **26**, 787 (2000).
[23] W. Treytl and K. Valli, Nucl. Phys. A **97**, 405 (1967).
[24] A. N. Andreyev *et al.*, Phys. Rev. C **79**, 064320 (2009).
[25] A. N. Andreyev *et al.*, Eur. Phys. J. A. **18**, 39 (2003).
[26] J. O. Rasmussen, Phys. Rev. **113**, 1593 (1959).

[27] P. Möller, J. R. Nix, and K.-L. Kratz, At. Data Nucl. Data Tables **66**, 131 (1997).
[28] M. Nyman, Research Report No. 12, Department of Physics, University of Jyväskylä, 2009.
[29] V. Paar, Nucl. Phys. A **331**, 16 (1979).
[30] R. B. Taylor *et al.*, Phys. Rev. C **59**, 673 (1999).
[31] A. N. Andreyev *et al.*, Phys. Rev. C **73**, 024317 (2006).